

HIGH-VELOCITY HCO^+ EMISSION FROM L1551 IRS 5: EVIDENCE FOR WIND-CLOUD INTERACTIONS

ALEXANDER RUDOLPH¹

Department of Astronomy, University of Maryland, College Park MD 20742

Received 1991 August 20; accepted 1992 July 21

ABSTRACT

HCO^+ ($J = 1 \rightarrow 0$) observations were made of L1551 IRS 5 to search for high-velocity and stationary emission associated with the bipolar outflow and the optical jet from this object. Aperture synthesis maps ($8'' \times 10''$ resolution) of this region reveal a bright blue emission wing extending from -40 to 0 km s^{-1} , coming from IRS 5; there is no other high-velocity gas seen in the region. This HCO^+ gas has more than enough momentum flux to drive the observed CO flow and is likely gas entrained by the neutral wind from IRS 5 as it passes through the surrounding cloud.

High-velocity-resolution maps of the same region reveal a number of stationary clumps associated with IRS 5, including a ridge of dense gas elongated perpendicular to the outflow. This ridge is the same one seen by Sargent et al. (1988) in C^{18}O emission. Comparison of the HCO^+ and C^{18}O emission strengths shows that the HCO^+ abundance in this dense ridge is 8–25 times lower than quiescent cloud values.

Two clumps of stationary HCO^+ emitting gas are seen in the direction of the blueshifted portion of the CO flow, on either side of the optical jet from IRS 5. These stationary clumps resemble those found by Rudolph & Welch (1988) downwind from the HH objects HH 7–11 and may be the material against which the wind from IRS 5 is being shocked, producing the optical jet. These clumps are likely part of a larger structure, possibly the walls of a cavity swept out by the wind from IRS 5.

Subject headings: stars: formation — stars: individual: L1551 IRS 5 — ISM: jets and outflows — radio lines: molecular: circumstellar

1. INTRODUCTION

Since the discovery of bipolar outflows, first seen around the young stellar object L1551 IRS 5 (Snell, Loren, & Plambeck 1980), one of the central problems in understanding these flows has been finding a source of momentum flux sufficient to drive the observed CO flows (Lada 1985). This problem was solved for the source HH 7–11 by the discovery of a fast ($v = 170 \text{ km s}^{-1}$), neutral wind with sufficient mass loss to drive the observed CO flow in this source (Lizano et al. 1988). In addition, Lizano et al. observed HCO^+ emission from HH 7–11 with a blue wing out to -100 km s^{-1} , and with an HCO^+ abundance enhanced by a factor of 40 or more relative to HCO^+ abundances found in quiescent molecular clouds (Vogel et al. 1984; Irvine, Goldsmith, & Hjalmarson 1987; Blake et al. 1987). They suggested that this gas was swept up from the surrounding gas by the fast neutral wind. Lizano et al. (1988) also made a marginal detection of $+50 \text{ km s}^{-1}$ H I gas from L1551. More recently, Giovanardi et al. (1992) have made a clear detection of redshifted H I emission from L1551 with velocities out to $+150 \text{ km s}^{-1}$.

In order to search for high-velocity gas and to look for stationary gas associated with the L1551 optical jet, interferometric HCO^+ observations, with both low- and high-velocity resolution, were made of the region surrounding IRS 5. This Letter reports the successful discovery of -50 km s^{-1} gas from IRS 5 as well as stationary clumps of material surrounding the L1551 optical jet.

2. OBSERVATIONS

Observations of the HCO^+ ($J = 1 \rightarrow 0$) transition (89.18852 GHz) were made with the Hat Creek millimeter

interferometer² in two periods, the first between 1988 December and 1989 April, and the second between 1990 May and 1990 August. The observations include eight configurations of the three 6.1 m antennas, with projected baselines from 6 to 120 m E–W and 90 m N–S. Observations were made of two fields, each 2.3 in diameter, one field centered on the pre-main-sequence star L1551 IRS 5, the other field centered on HH 29. The total integration time on each field was about 60 hr.

A 512 channel digital correlator (Urry, Thornton, & Hudson 1985) was used to obtain cross-correlation spectra with both high- and low-velocity resolution. Sixty-four 0.525 km s^{-1} wide channels were centered on 7 km s^{-1} , the cloud velocity. An additional 107 channels, with a velocity resolution of 2.1 km s^{-1} , were configured to give velocity coverage from -166 to 59 km s^{-1} , to look preferentially for blueshifted gas. The correlator was configured so that the lower sideband of the first local oscillator covered the ($2_2 \rightarrow 1_1$) transition of SO at 86.9355 GHz. No SO emission was found.

The point sources 0234 + 282, PK 0420, and 0528 + 134 were used as phase references. From the phase stability we estimate our absolute position accuracy to be approximately $1''$. Observations of Venus and Mars were used for absolute flux calibration using brightness temperatures from Ulich (1981). The absolute flux scale is accurate to about 20%. System temperatures ranged from 300 to 1000 K SSB scaled above the atmosphere, with a weighted average of 540 K for all the data. The rms sensitivity in a single 0.525 km s^{-1} channel is 1.2 K.

The visibility data were convolved onto a grid and Fourier-transformed and CLEANed to produce naturally weighted maps. The synthesized beam was $10'' \times 8''$. Due to the inability

² The Hat Creek millimeter interferometer is operated by the Berkeley-Illinois-Maryland Association with support from the National Science Foundation.

¹ Present address: NASA/Ames Research Center, Mail Stop 245-6, Moffett Field, CA 94035.

of the interferometer to measure uv spacings smaller than one antenna diameter ($6.1 \text{ m} = 1815 \lambda$), structures larger than approximately $60''$ were poorly sampled and are not well represented in the maps.

3. RESULTS

Figure 1 shows an integrated HCO^+ map ($v = 4.6\text{--}7.8 \text{ km s}^{-1}$) overlaid on an $[\text{S II}]$ image of the L1551 optical jet (Stocke et al. 1988). The HCO^+ map was made by averaging the narrow-velocity channels with velocities from 4.900 to 7.525 km s^{-1} , rejecting negative flux below a 2σ cutoff (2.3 K). The letters A–E label the five peaks of emission which had signal in a single channel above a 4σ level (4.6 K). The cross indicates the position of L1551 IRS 5.

Clump A refers to the ridge of emission centered $3''$ southeast of IRS 5, elongated along a position angle of 160° , roughly perpendicular to the L1551 outflow. The ridge is $23''$ in length (3700 AU at a distance of 160 pc) and is unresolved perpendicular to its extent. These characteristics exactly match those of the C^{18}O ridge seen by Sargent et al. (1988), suggesting that the HCO^+ emission is coming from the same gas. A position-velocity cut through this ridge shows no evidence for systematic motions, such as rotation.

Clumps C and D, which are spatially unresolved in this map, are clearly associated with the optical jet seen in $[\text{S II}]$. Extending the line of the jet shows that the jet passes between the two clumps.

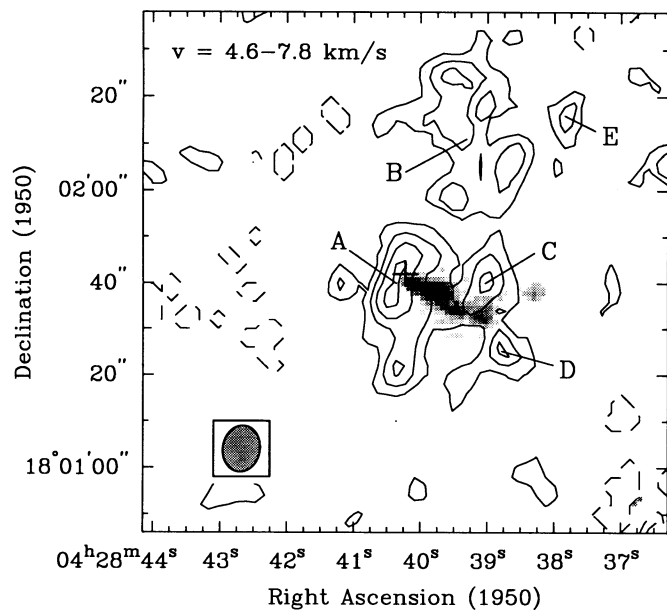


FIG. 1.—Average HCO^+ emission ($v = 4.6\text{--}7.8 \text{ km s}^{-1}$) near L1551 IRS 5, overlaid on a CCD image of $[\text{S II}]$ emission from the region (Stocke et al. 1988). The HCO^+ map was made by averaging six channels showing emission greater than 5 times the rms in a single map (1.2 K), but excluding negative signals below -2σ (-2.3 K). The contours levels are $(-3, -2, 2, 3, 4, 5) \times 0.5 \text{ K}$ (1σ). $1 \text{ K} = 0.5 \text{ Jy beam}^{-1}$. Dashed contours are negative. The cross marks the radio position of IRS 5. The HCO^+ peaks labeled A–E all contain signal above the 4σ level (4.6 K) in at least one channel (see Fig. 2). Clump A refers to the entire ridge of emission near IRS 5, at position angle 160° , and clump B refers to the extended emission northwest of IRS 5. Clumps C–E refer to unresolved clumps of HCO^+ emission. The synthesized beam ($10'' \times 8''$ at -10°) is displayed in the lower left-hand corner of the plot. $10''$ corresponds to $2.4 \times 10^{16} \text{ cm} = 0.008 \text{ pc}$ at a distance to L1551 of 160 pc .

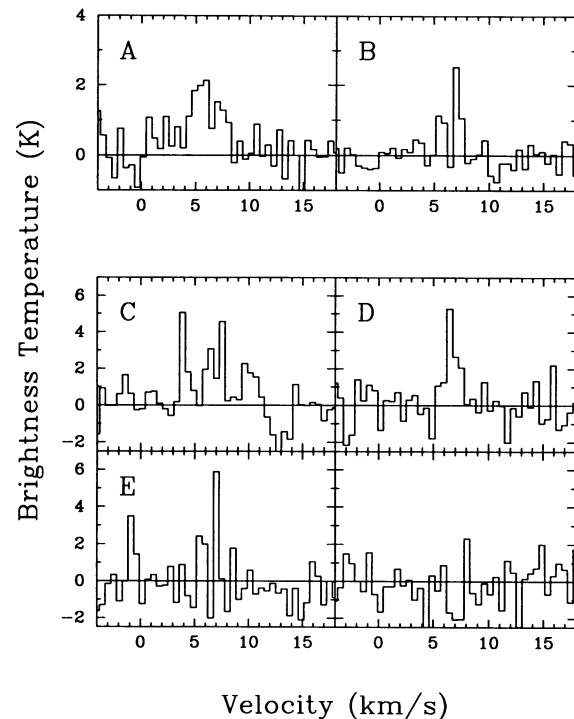


FIG. 2.—Spectra of the five HCO^+ clumps (A–E) marked in Fig. 1, plus a spectrum of blank sky for comparison. Note that the temperature scale for clumps A and B is different from that of the other clumps. The spectra for clumps A and B are averaged over boxes of size $22'' \times 14''$ and $40'' \times 24''$, respectively, whereas the spectra of clumps C–E and for the region of blank sky are peak brightness temperatures in a single beam. Therefore, the noise levels in the spectra of clumps A and B are lower than in the spectra of clumps C–E, and they differ from each other as well.

Figure 2 shows the spectra of the clumps A–E, along with a spectrum of a blank region of sky for comparison. The spectra of clumps A and B show average brightness temperature over the entire clump, whereas the spectra of clumps C, D, and E show the peak brightness temperature of these unresolved clumps. Note that the temperature scale in the plot of clumps A and B differs from that of clumps C–E. The linewidth of clump A is clearly wider than for clumps B–E, as would be expected for circumstellar material. Table 1 lists the average brightness for each clump, along with the size of the box, for clumps A and B, over which the brightness was averaged.

TABLE 1
 HCO^+ EMISSION FROM L1551

Clump (1)	T_b^a (2)	Box Size (3)	$N(\text{HCO}^+)$ (4)
A	2.1	$22'' \times 14''$	2×10^{13}
B	0.9	$40'' \times 24''$	$> 3 \times 10^{12}$
C	1.7	...	$> 1 \times 10^{13}$
D	1.9	...	$> 6 \times 10^{12}$
E	2.9	...	$> 5 \times 10^{12}$
HV	0.6	...	6×10^{13}

^a These temperatures are the average brightness temperature over the velocity range $4.6\text{--}7.8 \text{ km s}^{-1}$. For clumps A and B these brightness temperatures are also averaged over the boxes listed in col. (3). For clumps C–E and HV, these are brightness temperatures in the $10'' \times 8''$ beam.

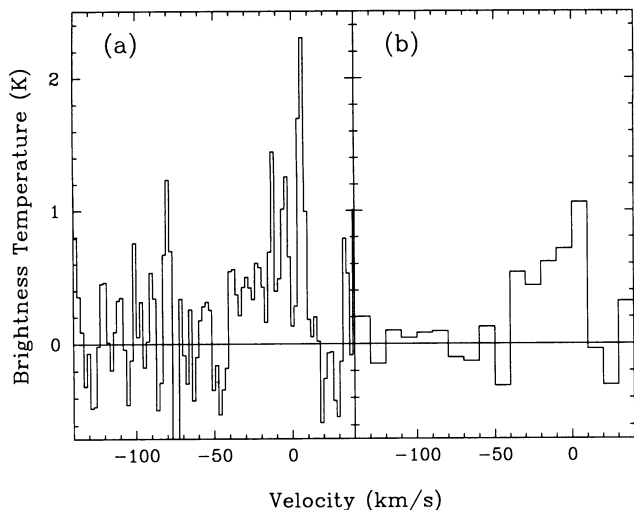


FIG. 3.—(a) Low-velocity resolution (2.1 km s⁻¹) HCO^+ spectrum of L1551 IRS 5. Note the broad blue wing. (b) The same spectrum taken with 10 km s⁻¹ channels, to improve signal-to-noise ratio. The blue wing is now quite prominent.

In addition to the narrow velocity channels, observations were made with wide-velocity channels (2.1 km s⁻¹ width), covering a much wider velocity range (−160 to 60 km s⁻¹). Figure 3a shows a spectrum of L1551 IRS 5 in these wider channels. The channels from −40 to 0 km s⁻¹ are clearly elevated above zero. To improve the signal-to-noise ratio in this spectrum, maps with 10 km s⁻¹ width were made, and a spectrum of IRS 5 was again taken. This spectrum is shown in Figure 3b. The blueshifted HCO^+ wing now clearly stands out above the noise level, confirming that this emission is real. The wing emission is roughly constant with velocity and has an average brightness of 0.6 K (see Table 1). A map of the channels from −40 to 0 km s⁻¹ reveals that this emission is unresolved and comes only from a region around IRS 5 smaller in extent than the 10'' beam (2×10^{16} cm). There is no evidence in the spectrum for redshifted gas.

Observations were made of HCO^+ emission near the HH object HH 29, but no emission was seen at any velocity above a brightness of 3.5 K (3 σ) in the narrow-velocity channels, and above a brightness of 1.2 K (3 σ) in the wide-velocity channels.

4. DISCUSSION

4.1. High-Velocity Gas

The blueshifted wing seen in Figure 3 has a roughly constant brightness temperature of 0.6 K, from 0 to −40 km s⁻¹, blueshifted 10 to 50 km s⁻¹ from the cloud velocity of 7 km s⁻¹ (Snell et al. 1980). The broad linewidth makes it extremely unlikely that this emission is coming from a single, fast-moving clump. Rather, the observed rectangular line shape is consistent with emission from a constant velocity, spherically diverging, fast wind, regardless if the sphere is complete or not (Bertout & Magnan 1987; Lizano et al. 1988). The ratio of radial to tangential velocities of the Herbig-Haro objects in the flow implies that the wind is being observed at an angle of 75° from the line of sight (Strom, Grasdalen, & Strom 1974; Cudworth & Herbig 1979; Snell & Schloerb 1985), while the opening angle of the flow is approximately 20° (Snell et al. 1980). Thus, for a maximum observed velocity of 50 km s⁻¹, the implied maximum velocity of the gas is 90 km s⁻¹ (see Lizano et al. for geometrical details).

The HCO^+ gas in this wing could be part of a wind from IRS 5 which is driving the CO outflow, or it could be material swept up as the wind interacts with the surroundings. H I emission has been observed in L1551 at velocities up to +150 km s⁻¹ (Giovanardi et al. 1992; Lizano et al. 1988), corresponding to a deprojected velocity of the neutral wind of 260 km s⁻¹. In these observations, the blueshifted portion of the spectrum is contaminated by Galactic H I emission along the line of sight. However, if one makes the plausible assumption that the neutral wind is symmetric in velocity (as is seen in HH 7–11), then the HCO^+ gas has a velocity lower than that of the neutral wind, but higher than that of the large-scale CO flow (Snell & Schloerb 1985). This intermediate velocity suggests that the HCO^+ is material entrained by the wind, not material in the neutral wind. This result is similar to that of Lizano et al. (1988) who, in addition to detecting high-velocity (± 170 km s⁻¹) H I gas, detected intermediate-velocity (−100 km s⁻¹) blueshifted HCO^+ emission in a 20'' beam centered on SVS 13 (the star driving the HH 7–11 outflow).

The mass and momentum in the HCO^+ gas can be calculated from the observed emission strength, if one assumes that the gas is molecular, that the emission is optically thin, and that the wind is dense enough to thermalize the gas at a temperature T . Under these assumptions, the mass and momentum in this gas is (including helium)

$$M = \left(\frac{0.0013}{\eta} \right) \left(\frac{T}{50} \right) \int T_b dv M_\odot,$$

and

$$P = \left(\frac{0.042}{\eta} \right) \left(\frac{T}{50} \right) \int T_b dv M_\odot \text{ km s}^{-1},$$

where the brightness temperature, T_b , is measured in K; the velocity width of the line, dv , is measured in km s⁻¹; and where the abundance of HCO^+ relative to H_2 is $2 \times 10^{-9}\eta$, with $\eta = 1\text{--}4$ for quiescent molecular clouds (Vogel et al. 1984; Irvine et al. 1987; Blake et al. 1987). In L1551, the integrated line strengths is $\int T_b dv = (0.6 \text{ K})(40 \text{ km s}^{-1}) = 24 \text{ K km s}^{-1}$, so the mass and momentum of this gas is

$$M = \left(\frac{0.032}{\eta} \right) \left(\frac{T}{50} \right) M_\odot,$$

and

$$P = \left(\frac{1.0}{\eta} \right) \left(\frac{T}{50} \right) M_\odot \text{ km s}^{-1}.$$

Moriarty-Schieven & Snell (1988) measured the momentum in the blue wing of the CO outflow, corrected for optical depth, and found it to be $8.7 M_\odot \text{ km s}^{-1}$. Since the crossing time for the gas detected in HCO^+ is less than 130 yr, 700 times shorter than for the CO outflow, the high-velocity gas carries, on a 5'' scale, (80/ η) times more momentum flux than the CO flow, at a temperature of 50 K. Thus, this gas has more than enough momentum flux to drive the observed CO flow.

The large implied overabundance of momentum flux in the HCO^+ gas, when compared to the CO outflow, can be explained in at least two ways. First, the HCO^+ abundance might be enhanced compared to values found in quiescent clouds ($\eta \geq 1\text{--}4$). Second, the wind might be sporadic, so that the CO gas contains momentum collected over many violent outbursts rather than from a single continuous flow.

In the first case, since the average temperature in this gas is unlikely to be much lower than 50 K (Ruden, Glassgold, & Shu 1990), then if the flow is continuous, the HCO^+ abundance must be strongly enhanced. DeNoyer & Frerking (1981) found evidence that the HCO^+ abundance in the shocked molecular gas associated with the supernova remnant IC 443 was enhanced by a factor of 10. Cohen et al. (1988) detected $63\ \mu\text{m}$ $[\text{O I}]$ emission in a $44''$ beam centered on IRS 5 which they interpret as emission from shocks in the optical jet emanating from IRS 5. Thus, shocks occurring when the fast wind from IRS 5 encounters the surrounding material and entrains the HCO^+ gas detected here, might provide a mechanism for enhancing the HCO^+ abundance in this entrained gas.

In the second case, if the HCO^+ abundance is *not* enhanced, then the fraction of time during which the wind blows would have to be less than $1/80$ to account for the momentum flux of the HCO^+ gas, suggesting that estimates of the lifetime of the CO flow might be too high.

The HCO^+ spectrum presented here is clearly asymmetric. However, due to the modest signal-to-noise ratio of these observations and the bias of the correlator passband toward blueshifted velocities, the existence of redshifted HCO^+ emission cannot be ruled out.

4.2. Circumstellar Material

Clump A in Figure 1 is an extended ridge of material, $23''$ in extent along a position angle of 160° , and unresolved perpendicular to its extent. This ridge coincides in velocity, size, and orientation with the ridge of C^{18}O emission seen by Sargent et al. (1988) around IRS 5 in their lower resolution maps. Thus, the HCO^+ -emitting gas is identified with this C^{18}O ridge.

Assuming that the HCO^+ emission is optically thin and is coming from gas in local LTE at 50 K (Butner et al. 1991), the column density implies from the integrated HCO^+ line strength is $2 \times 10^{13}\ \text{cm}^{-2}$ (see Table 1). The column density of H_2 implied by the C^{18}O observations is $2\text{--}7 \times 10^{22}$; thus, the implied HCO^+ abundance is $3\text{--}10 \times 10^{-10}$. Although this abundance determination is very uncertain, this value is 8–25 times lower than the value found in quiescent dark clouds, such as TMC-1 (Blake et al. 1987) but similar to the value found in a ridge of material around HH 34 IR (Rudolph & Welch 1992).

4.3. Stationary Material near the Optical Jet

Clumps C and D are both stationary clumps in close proximity to the optical jet emanating from L1551 IRS 5 (see Fig.

1). The spectrum of clump D is rather simple, while the spectrum of clump C is somewhat more complicated (see Fig. 2), consisting of a number of narrow velocity spikes over several kilometers per second. Both clumps resemble the stationary clumps seen by Rudolph & Welch (1988) near HH 7–11, which were interpreted as the dense cloudlets against which the high-velocity wind from SVS 13 was being shocked, forming HH 7–11.

Lower limits to the HCO^+ column densities in these clumps (as well as in clumps B and E) were determined by assuming that the emission is optically thin, and from gas in LTE at the average temperature of the cloud, 15 K (Snell 1981; Torrelles et al. 1983; see Table 1). If the emission is optically thick, or if the gas is much hotter than 15 K, then the column densities could be higher.

Although clumps C and D do not form a nice structure like the walls of the hollow cavity seen near HH 34 (Rudolph & Welch 1992), the clumps do appear on either side of the line formed by the optical jet from IRS 5. This morphology suggests that the HCO^+ clumps may be part of the cavity which has formed as the fast neutral wind from IRS 5 flows into the surroundings. This suggestion is borne out by considering the kinematics of the two clumps which both have velocities very near the cloud velocity. Rudolph (1988) showed that clumps of density $10^5\ \text{cm}^{-3}$ (the critical density of HCO^+) will be accelerated by a $150\ \text{km s}^{-1}$ wind of density $100\ \text{cm}^{-3}$ to a velocity greater than $1\ \text{km s}^{-1}$ in less than 250 yr, much shorter than the lifetime of the outflow (Moriarty-Schieven & Snell 1988). Thus, the low velocities of these clumps suggest that they are not isolated structures, but are part of a larger structure, such as the walls of a cavity blown by the neutral wind from IRS 5. If this suggestion is correct, then the large CO cavity detected by Moriarty-Schieven & Snell (1988) continues down to very small scales ($\lesssim 0.01\ \text{pc}$).

I would like to thank Pat Hartigan for providing a FITS version of the S II image from Stocke et al. (1988), and Jim Morgan for developing the program WIP which generated the figures in this paper. I would also like to thank Jack Welch for many helpful suggestions which improved the paper. Partial support for this research was provided by NSF grants AST-87 14721 and AST-91 0306, and by the State of Maryland through its contributions to the Laboratory for Millimeter-Wave Astronomy.

REFERENCES

- Bertout, C., & Magnan, C. 1987, *A&A*, 183, 319
 Blake, G. A., Sutton, E. C., Masson, C. R., & Phillips, T. G. 1987, *ApJ*, 315, 621
 Lada, C. J. 1985, *ARA&A*, 23, 267
 Butner, H. M., Evans, N. J., II, Lester, D. F., Levreault, R. M., & Strom, S. E. 1991, *ApJ*, 376, 636
 Cohen, M., Hollenbach, D. J., Haas, M. R., & Erickson, E. F. 1988, *ApJ*, 329, 863
 Cudworth, K. M., & Herbig, G. H. 1979, *AJ*, 84, 548
 DeNoyer, L. K., & Frerking, M. A. 1981, *ApJ*, 246, L37
 Giovanardi, C., Lizano, S., Natta, A., Evans, N. J., II, & Heiles, C. 1992, *ApJ*, 397, 214
 Irvine, W. M., Goldsmith, P. F., & Hjalmarson, A. 1987, in *Interstellar Processes*, ed. D. J. Hollenbach & H. A. Thronson, Jr. (Dordrecht: Reidel), 561
 Lada, C. J. 1985, *ARA&A*, 23, 267
 Lizano, S., et al. 1988, *ApJ*, 328, 763
 Moriarty-Schieven, G. H., & Snell, R. L. 1988, *ApJ*, 332, 364
 Ruden, S. P., Glassgold, A. E., & Shu, F. H. 1990, *ApJ*, 361, 546
 Rudolph, A. 1988, Ph.D. thesis, Univ. of Chicago
 Rudolph, A., & Welch, W. J. 1988, *ApJ*, 326, L31
 ———. 1992, *ApJ*, 395, 488
 Sargent, A. I., Beckwith, S., Keene, J., & Masson, C. 1988, *ApJ*, 333, 936
 Snell, R. L. 1981, *ApJS*, 45, 121
 Snell, R. L., Loren, R. B., & Plambeck, R. L. 1980, *ApJ*, 239, L17
 Snell, R. L., & Schloerb, F. B. 1985, *ApJ*, 295, 490
 Stocke, J. T., Hartigan, P. M., Strom, S. E., Strom, K. M., Anderson, E. R., Hartmann, L. W., & Kenyon, S. J. 1988, *ApJS*, 68, 229
 Strom, S. E., Grasdalen, G. L., & Strom, K. M. 1974, *ApJ*, 191, 111
 Torrelles, J. M., Rodríguez, L. F., Cantó, J., Carral, P., Marcaide, J., Moran, J. M., & Ho, P. T. P. 1983, *ApJ*, 274, 214
 Ulich, B. L. 1981, *AJ*, 86, 1619
 Urry, W. L., Thornton, D. D., & Hudson, J. A. 1985, *PASP*, 97, 745
 Vogel, S. N., Wright, M. C. H., Plambeck, R. L., & Welch, W. J. 1984, *ApJ*, 283, 655